JOURNAL OF AIRCRAFT
Vol. 35, No. 6, November–December 1998

Neural Network and Regression Approximations in High-Speed Civil Aircraft Design Optimization

Surya N. Patnaik*
Ohio Aerospace Institute, Brook Park, Ohio 44142-1068
and
James D. Guptill,† Dale A. Hopkins,‡ and Thomas M. Lavelle§
NASA Lewis Research Center, Cleveland, Ohio 44135-3191

Nonlinear mathematical-programming-based design optimization can be an elegant method. However, the calculations required to generate the merit function, constraints, and their gradients, which are frequently required, make the process computationally intensive. The computational burden can be substantially reduced by using approximating analyzers derived from an original analyzer utilizing neural networks and linear regression methods. The experience gained from using both of these approximation methods in the design optimization of a high-speed civil transport aircraft is the subject of this paper. The NASA Langley Research Center's Flight Optimization System was selected for the aircraft analysis. This software was exercised to generate a set of training data with which a neural network and regression method were trained, thereby producing the two approximating analyzers. The derived analyzers were coupled to the NASA Lewis Research Center's CometBoards test bed to provide the optimization capability. Both approximation methods were examined for use in aircraft design optimization, and both performed satisfactorily. The CPU time for solution of the problem, which had been measured in hours, was reduced to minutes with the neural network approximation and to seconds with the regression method. Instability encountered in the aircraft analysis software at certain design points was also eliminated. However, there were costs and difficulties associated with training the approximating analyzers. The CPU time required to generate the I/O pairs and to train the approximating analyzers was seven times that required for solution of the problem.

Nomenclature

bw = bandwidth
g = constraints
l = length
T = temperature
t = thrust
v = velocity
w = weight factor
$\boldsymbol{x}$ = design variables
y = approximating function
α = clustering algorithm control parameter
β = regression coefficients
γ = merit function component
ς = kernel function

Introduction

INTENSIVE computation can be a serious deficiency in an otherwise elegant nonlinear mathematical-programming-based design optimization method. In typical structural design applications, most of the computations, often more than 99% of the total calculations, can be traced to the analyzer.[1] That is, reanalysis and sensitivity calculations consume the bulk of the computation time in design optimization. To reduce the computational burden, two approximation methods, regression analysis and neural networks, have been incorporated into the NASA Lewis Research Center's design test bed CometBoards[1–3] (comparative evaluation test bed of optimization and analysis routines for the design of structures). Both approximation methods provide the reanalysis and design sensitivity information that is usually required during optimization. Approximation augmentation, which includes a strategy to select training pairs, has broadened the scope of CometBoards; thus, a design problem can be solved by using three different analyzers—the original analyzer or one of the two derived analyzers that are based on regression and neural networks.

The example of a high-speed civil transport (HSCT) aircraft is considered to examine the performance of approximation methods in design optimization. The NASA Langley Research Center's Flight Optimization System (FLOPS),[4,5] which is well known in industry, was chosen as the aircraft analyzer. This analyzer is not just computationally intensive; it can also become unstable at certain design points, thereby requiring that the optimization process be restarted. Moreover, an optimum benchmark solution established for the HSCT aircraft problem from results generated previously with the FLOPS analyzer by NASA Langley and Lewis Research Centers, and industry can be a useful solution against which the results obtained with the approximation methods can be compared. CometBoards, which includes an approximation module containing regression analysis as well as neural networks, has been soft-coupled to the FLOPS analyzer. The CometBoards–FLOPS combined software can optimize an HSCT aircraft by using any one of the three analyzers—the original FLOPS code, or the derived regression or neural network models. This paper presents optimal solutions that were generated for the HSCT aircraft by using all three analyzers. Results are examined to assess the

Received Feb. 7, 1998; revision received June 8, 1998; accepted for publication June 30, 1998.

*Engineer, 22800 Cedar Point Road; currently at NASA Lewis Research Center, M/S 49-8, Materials and Structures, Cleveland, OH 44135-3191. Associate Fellow AIAA.

†Mathematician, Computational Sciences Branch, 21000 Brookpark Road.

‡Engineer, Machine Dynamics Branch, 21000 Brookpark Road. Senior Member AIAA.

§Engineer, Propulsion System Analysis Office, 21000 Brookpark Road.

performance of the neural network and regression methods in the design of an HSCT aircraft system, which is the primary objective of this paper. The evaluation quantifies the computational benefit, the payoff from the use of closed-form vs numerical sensitivities in design calculations, and the training and use ranges. In specific terms, the deviation in the aircraft weight and behavior constraints, and their sensitivity, are investigated for analysis as well as design. The computational efficiency achieved by using approximation methods in design optimization is examined by comparing CPU solution times.

This paper is organized as follows: an overview of the CometBoards design test bed, a brief description of the aircraft analyzer FLOPS, a strategy to generate the input portion of the I/O pairs for training both approximating analyzers, a brief description of regression analysis and neural networks, a definition of the design problem and the benchmark solution, generation of the I/O pairs for this problem, representative response prediction through the approximation methods, the performance of both approximation methods in predicting the behavior parameters of the aircraft, their performance during design optimization, and conclusions.

CometBoards: A Design Test Bed

Our earlier research to compare alternate optimization algorithms and different analysis methods for structural design applications has grown into a multidisciplinary design test bed that is still referred to by its original acronym, CometBoards. The modular organization of CometBoards (Fig. 1) allows innovative methods to be quickly validated through the integration of new programs into its existing modules. Optimizers and analyzers are two important modules of CometBoards. The optimizer module includes a number of algorithms, such as the fully utilized design and optimality criteria methods,[6] the method of feasible directions,[7] the modified method of feasible directions,[8] three different sequential quadratic programming techniques,[9–11] the sequential unconstrained minimizations technique,[12] sequential linear programming,[7] a reduced gradient method,[13] etc. Likewise, the analyzer module includes COSMIC/NASTRAN,[14] the nonlinear analyzer MHOST,[15] the U.S. Air Force ANALYZE/DANALYZE,[16] IFM/ANALYZERS,[17] the aircraft flight optimization analysis code FLOPS,[5] the NASA Engine Performance Program NEPP,[18] and others. Some of the other unique features of CometBoards include a cascade optimization strategy, design variable and constraint formulations, a global scaling strategy, analysis and sensitivity approximations through regression and neural networks, and substructure optimization on sequential as well as parallel computational platforms.[19] CometBoards has provisions to accommodate up to 10 different disciplines, each of which can have a maximum of five subproblems. The test bed can optimize a large system, which can be defined in as many as 50

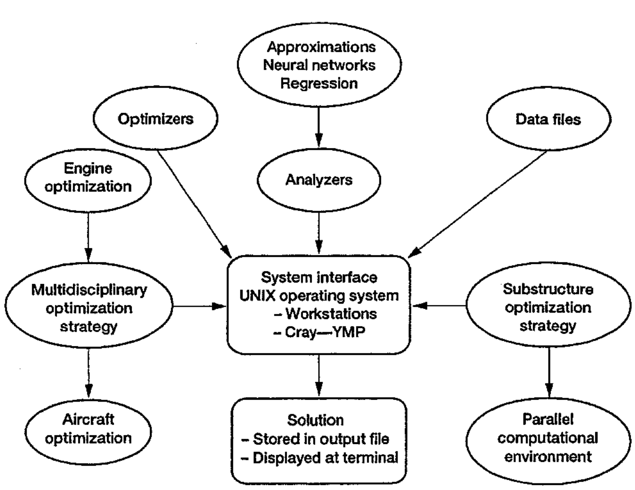

Fig. 1 Organization of CometBoards test bed.

different subproblems. Alternatively, a component of a large system can be optimized to improve an existing system. The design test bed has been successfully used to solve a number of problems, such as the structural design of space station components; the design of nozzle components for air-breathing engines; and the configuration design of subsonic and supersonic aircraft, mixed flow turbofan engines, and wave rotor concepts in engines. CometBoards has over 50 numerical examples in its test bed. It is written in Fortran 77, except for the neural network code, Cometnet,[20] which is written in C++. The process of integrating this C++ code into the CometBoards Fortran 77 code is referred to as soft-coupling. Soft-coupling is achieved by first generating an executable file from the Cometnet C++ source code; then Cometnet is invoked from CometBoards through a system call. Information is exchanged between the two programs through data files. At present CometBoards is available on UNIX-based Cray and Convex computers and on Iris and Sun workstations. CometBoards is continuously being improved to increase its reliability and robustness for optimization at system as well as component levels. This paper emphasizes the approximation module of CometBoards, which includes regression analysis and neural network approximations for the design optimization of an HSCT aircraft.

FLOPS: An Aircraft Analyzer

Aircraft design was formulated as a nonlinear programming problem with a set of design variables to optimize a merit function under a set of behavior constraints. The FLOPS analyzer evaluated the performance parameters of an advanced aircraft to generate the constraints and merit function. By soft-coupling NASA Lewis Research Center's CometBoards and NASA Langley Research Center's FLOPS, the design problem could be set up and solved without major modification to either code. The design problem was solved by using the CometBoards–FLOPS combined capability.

The FLOPS analyzer has eight disciplines: weight estimation, aerodynamic analysis,[21,22] engine cycle analysis,[23–25] propulsion data interpolation, mission performance, airfield length requirements for takeoff and landing, noise footprint calculations,[26] and cost estimation.[27–32] The FLOPS analyzer allows selection of the following free variables for the purpose of optimization: 1) ramp weight, 2) wing aspect ratio, 3) engine thrust, 4) taper ratio of the wing, 5) reference wing area, 6) quarter-chord sweep angle of the wing, 7) wing thickness to chord ratio, 8) cruise Mach number, 9) cruise altitude, 10) engine design point turbine entry temperature, 11) overall pressure ratio, 12) bypass ratio for turbofan engines, 13) fan pressure ratio for turbofan engines, and 14) engine throttle ratio (defined as the ratio of maximum allowable tubine inlet temperature divided by the design point turbine inlet temperature). For the HSCT problem, the free variables were separated into a set of six active design variables and a set of eight passive design variables.

For the purpose of optimization, the composite merit function available in FLOPS can be written as

$$\text{Obj} = \sum_{k=1}^{7} w_k \gamma_k \tag{1}$$

where Obj represents the merit function, w_k represents the kth weight factor, and the parameter γ_k can be selected from the following list: 1) gross takeoff weight of the aircraft, 2) mission fuel, 3) the product of the Mach number times the ratio of lift-to-drag, 4) range, 5) cost, 6) specific fuel consumption, and 7) NO_x emissions. For the HSCT problem, the gross takeoff weight was selected as the merit function by setting $w_1 = 1.0$ and the other weight factors to zero.

Behavior constraints can be imposed on the 1) missed approach climb gradient thrust, 2) second-segment climb thrust,

3) landing approach velocity, 4) takeoff field length, 5) jet velocity, 6) compressor discharge temperature, 7) total usable fuel weight, 8) range of the flight, 9) landing field length, 10) aspect ratio (defined as the ratio of bypass area to the core area of a mixed flow turbofan engine), 11) engine-throttle ratio, 12) specific fuel consumption, 13) compressor discharge pressure, and 14) excess fuel, etc. Only the first six constraints were imposed in the HSCT problem.

The design space of an aircraft optimization problem can be distorted because both design variables and constraints vary over a wide range. For example, an engine thrust design variable (which is measured in kilopounds, e.g., 40,000 lb), is immensely different from the bypass ratio variable (which is a small number, e.g., 0.5). Likewise, a landing velocity constraint in knots and a field length limitation in thousands of feet differ both in magnitude and in units of measure. In CometBoards the distortion is reduced by scaling the merit function, design variables, and constraints such that their normalized values are around unity.

Selection Strategy for Input Portion of I/O Pairs for Training

Both regression and neural network approximations require a set of I/O pairs for their training. The quality of the approximation depends on the selected set of design points used to generate the I/O pairs. Statisticians have long recognized the importance of the sample, the selection of which utilizes a design-of-experiments method. A strategy has been devised to generate a set of design variables that form the input portion of the training pairs. This strategy has two principal steps: 1) separation of the design space into subspaces, and 2) division of each design variable range into subintervals. The first step addresses the intrinsic coupling of design variables that can be inherent in large design problems. The second step allows a bias toward, e.g., the initial design or the bounds of the range. The output portion, representing the merit function and behavior constraints, is generated from the FLOPS analyzer for the specified input design variables.

The input variable selection strategy is illustrated by considering a design problem with six active variables (1–5 and 7) and one passive variable (6) as an example. The six active variables are separated into four related sets, designated by circled digits 1–4 in Fig. 2. The design variables are shown in braces: {4, 7}, {2}, {3, 5}, and {1, 2, 7} for sets 1 through 4, respectively. Their coupling and influence regions, shown in Fig. 2, are given in Table 1. Consider, e.g., set 3 with two influence regions (2 and 4, see Fig. 2). Response prediction for set 3 (with two active design variables of its own) will include those of its coupling regions (design variables 1, 2, 3, 5, and 7). These five variables will be perturbed by using the scheme described next, and in addition, other active variables may also undergo minor perturbations.

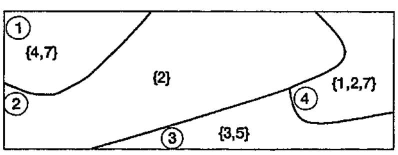

Fig. 2 Design variable sets with influence regions. Circled numbers represent sets; braced numbers are active design variables. Adjacent regions are coupling regions.

Consider a design variable in a set with initial design χ^i, upper bound χ^u, and lower bound χ^l. Divide the interval between the lower bound and the initial design, and that between the initial design and the upper bound, into n_{il} and n_{iu} subintervals, respectively. A bandwidth bw is assigned for the design variable that specifies the number of subintervals to be grouped together to form random perturbations. To illustrate the strategy for selecting the input portion of a set of I/O pairs, let us consider a simple example with two design variables. The perturbation scheme requires the following data for each variable:

1) Design variable 1: lower, initial, and upper bounds of, e.g., 0.05, 4.00, and 10.00, respectively.

2) Design variable 2: lower, initial, and upper bounds of, e.g., 0.50, 6.00, and 9.50, respectively.

Let us divide the intervals between the lower bound and the initial design into four subintervals. Likewise, divide the interval between the initial design and the upper bound into three subintervals. Assume a moderate clustering of subintervals by taking a bandwidth $bw = 3$. (There is no clustering when the bandwidth is unity.) Specify the number of perturbations for each subinterval as follows: for the four subintervals beginning from the initial design toward the lower bound, 15, 10, 2, and 6, and for the three subintervals from the initial design to the upper bound, 10, 4, and 8.

The input portion of the I/O pairs generated through the selection strategy is depicted in Fig. 3. There are 131 design points. The inner circle, with a radius of 2 centered on the initial design (4, 6), captures 31 design points, which corresponds to a density of 2.5 points per unit area. The annulus with radii of 2 and 3 also contains 31 design points, but is less dense with 2.0 points per unit area. The bias is not prominent in the pattern shown in Fig. 3 because of the simplicity of the problem. A different pattern for the input portion of the I/O pairs can be generated by changing the bandwidth, number of intervals, stations, and perturbations. The pattern can be improved interatively.

Linear Regression Analysis

The regression analysis available in CometBoards uses several basis functions. The basis functions can be selected from 1) a full cubic polynomial, 2) a quadratic polynomial, 3) a linear polynomial in reciprocal variables, 4) a quadratic polynomial in reciprocal variables, and 5) combinations thereof. Consider, for example, regression analysis of an n variable model with a combination of a cubic polynomial in design variables and a quadratic polynomial in reciprocal design variables. The regression function has the following explicit form

$$y(\boldsymbol{x}) = \beta_0 + \sum_{i=1}^{n} \beta_i x_i + \sum_{i=1}^{n}\sum_{j=i}^{n} \beta_{ij} x_i x_j + \sum_{i=1}^{n}\sum_{j=i}^{n}\sum_{k=j}^{n} \beta_{ijk} x_i x_j x_k + \sum_{i=1}^{n} \bar{\beta}_i \frac{1}{x_i} + \sum_{i=1}^{n}\sum_{j=i}^{n} \bar{\beta}_{ij} \frac{1}{x_i x_j} \tag{2}$$

The regression coefficients β are determined by using the linear least-squares approach incorporated in the double precision general matrix linear least-squares solver (DGELS) routine of the Lapack library.[33] The gradient matrix of the regression function with respect to the design variables is obtained in

Table 1 Design variable selection strategy

Related sets	Active design variables		Influence region		Variables in design zones	
	Number	Variables	Number	Sets	Number	Variables
1	2	4, 7	1	2	3	2, 4, 7
2	1	2	3	1, 3, 4	6	1, 2, 3, 4, 5, 7
3	2	3, 5	2	2, 4	5	1, 2, 3, 5, 7
4	3	1, 2, 7	2	2, 3	5	1, 2, 3, 5, 7

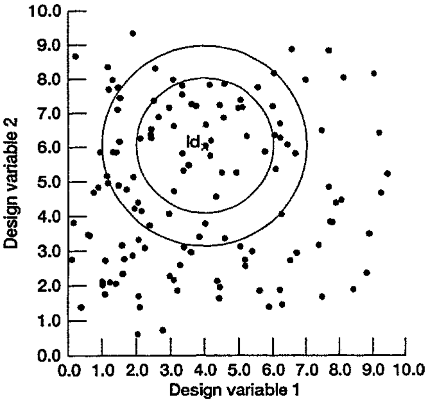

Fig. 3 Input portion of I/O pair for two design variables.

closed form. For the example with n variables, the gradient matrix for the regression function has the following form:

$$\nabla y = \begin{matrix} \dfrac{\partial}{\partial x_1} \\ \dfrac{\partial}{\partial x_2} \\ \vdots \\ \dfrac{\partial}{\partial x_n} \end{matrix} \; y \tag{3}$$

where

$$\frac{\partial y}{\partial x_l} = \beta_l + \sum_{i=1}^{n} \beta_{il} x_i + \beta_{ll} x_l + \sum_{i=1}^{n-1} \sum_{j=i+1}^{n} \beta_{ijl} x_i x_j + \sum_{i=1}^{n} \beta_{iil} x_i^2$$
$$+ \sum_{j=i}^{n} \beta_{ill} x_i x_l + \beta_{lll} x_l^2 - \frac{\bar{\beta}_l}{x_l^2} - \frac{1}{x_l^2} \sum_{i=1}^{n} \bar{\beta}_{il} \frac{1}{x_i} - \frac{\bar{\beta}_{ll}}{x_l^3} \tag{4}$$

and $\beta_{ij} = \beta_{ji}$ for $i > j$, $\beta_{ijk} = \beta_{ikj}$ for $j > k > i$, etc.

Once the regression coefficients have been obtained from the single training cycle, reanalysis and sensitivity calculations represented by Eqs. (2–4) require trivial computational effort. In regression analysis, the accuracy of the approximation function and its gradient can differ significantly near, as well as outside of, the boundary of the training domain. This deficiency, if any, in CometBoards can be reduced by selecting either closed-form or finite difference gradients, at the discretion of the user.

Neural Network Approximations

The neural network approximator available in CometBoards, Cometnet,[20] is a general-purpose, object-oriented neural network library that provides for both linear and nonlinear models. Cometnet is soft-coupled to the CometBoards test bed. The neural network capability provides both function values and their gradients. Cometnet approximates the function and its gradient with R kernel functions as follows:

$$y(\boldsymbol{x}) = \sum_{r=1}^{R} \sum_{i=1}^{n_r} w_{ri} \varsigma_{ri}(\boldsymbol{x}) \tag{5a}$$

$$\frac{\partial y(\boldsymbol{x})}{\partial x_l} = \sum_{r=1}^{R} \sum_{i=1}^{n_r} w_{ri} \frac{\partial \varsigma_{ri}(\boldsymbol{x})}{\partial x_l} \tag{5b}$$

where y is the functional approximation, $\boldsymbol{x}$ is the vector of independent variables, ς_{ri} represents R kernel functions, n_r represents the number of basis functions in a given kernel, and w_{ri} are the weight factors.

Cometnet permits approximations by using different kernels, which include linear, reciprocal, and polynomial, as well as Cauchy and Gaussian radial functions. A singular value decomposition algorithm,[34] for computing the weight factors in the approximating function, is used to train the network. A clustering algorithm is used to select suitable parameters for defining the radial functions. The clustering algorithm, in conjunction with an optimizer, seeks optimal values for the parameters over a range for the threshold parameter τ within its domain ($0 < \tau < 1$). A user-specified parameter α ($0 < \alpha < 2$) that controls the clustering algorithms is used to specify the relative radius of the Gaussian and Cauchy kernel functions. Increasing the value of the parameter can reduce the training error, but may increase the test error. The mean-square error during training is reduced by increasing the threshold, which corresponds to an increase in the number of basis functions. Overfitting is avoided with a competing complexity-based regularization algorithm.[35] The merit function and each of the constraint functions can be trained separately by using different basis functions.

Definition of the HSCT Aircraft Design Problem

The HSCT aircraft problem devised by NASA Langley Research Center was employed to examine the performance of the approximation methods for both analysis and optimization.[24] This supersonic aircraft was to be powered by four mixed-flow turbofan engines. The mission requirement of the aircraft is to carry 305 passengers at a cruise speed of Mach 2.4 for a range of 5000 n miles. The objective of the optimization was to determine the airframe–engine design combination that would meet these constraints with a minimum gross takeoff weight. A good match between the engine and airframe can be achieved by combining the engine parameters with the airframe variables. Six active design variables were selected to optimize the design. There were two airframe design variables, the engine thrust and the wing size, and four engine design parameters, the turbine inlet temperature, overall pressure ratio, bypass ratio, and fan pressure ratio. The turbine inlet temperature was limited to a maximum of 3560°R. The constraints imposed on the aircraft and engine were as follows: the takeoff and landing field lengths had to be less than 11,000 ft, the approach velocity had to be less than 160 kn; there had to be enough volume to carry all of the required fuel, there had to be enough engine thrust available to recover from a missed approach and execute a second-segment climb, the exit jet velocity had to be less than 2300 ft/s to limit engine noise, and the compressor discharge temperature had to be less than 1710°R.

To assess the performance of the approximation methods, the design space was divided into three subregions: the standard, wide, and restricted range. The range used to train the approximating analyzers is referred to as the standard range and designated with the letter "b" in Table 2. The wide range, designated by the letter "a," was defined as the range outside the training range. The restricted range, designated by the letter "c," is defined as the range inside the training range. The design variables, their ranges, and status (active or passive) are specified in Table 2.

The six behavior constraints, which are implicit functions of the design variables, were as follows:

1) Missed approach climb thrust t_c, which must be positive; it was normalized with respect to 10^6 lb:

$$g_1 = -(t_c/10^6) \leq 0$$

2) Second-segment climb thrust t_s, which must be positive; it was normalized with respect to 10^4 lb:

$$g_2 = -(t_s/10^4) \leq 0$$

Table 2 Design variables and their ranges for the HSCT aircraft

Number	Description	Status	Lower bound	Initial design	Upper bound
1	Ramp weight, lb	Passive	——	——	——
2	Wing aspect ratio	Passive	——	2.36	——
3	Engine thrust, lb	Active	30,000[a]	50,000[a]	70,000[a]
			36,000[b]	41,000[b]	45,000[b]
			40,500[c]	41,000[c]	41,500[c]
4	Taper ratio of wing	Passive		0.057	
5	Wing area, ft^2	Active	7,000[a]	8,000[a]	12,000[a]
			7,100[b]	8,100[b]	9,100[b]
			8,000[c]	8,100[c]	9,000[c]
6	Sweep angle, deg	Passive	——	62.22	——
7	Wing thickness-chord ratio	Passive	——	0.03	——
8	Cruise Mach number	Passive	——	2.4	——
9	Maximum cruise altitude, ft	Passive	——	70,000	——
10	Turbine entry temperature, °R	Active	2,300[a]	3,000[a]	3,560[a]
			2,300[b]	2,900[b]	3,500[b]
			2,850[c]	2,900[c]	3,000[c]
11	Overall pressure ratio	Active	15[a]	24[a]	30[a]
			18[b]	21[b]	25[b]
			20[c]	21[c]	22[c]
12	Bypass ratio	Active	0.10[a]	0.25[a]	0.8[a]
			0.25[b]	0.40[b]	0.8[b]
			0.39[c]	0.40[c]	0.5[c]
13	Fan pressure ratio	Active	1.2[a]	3.6[a]	4.8[a]
			2.6[b]	3.6[b]	4.6[b]
			3.5[c]	3.6[c]	3.8[c]
14	Engine throttle ratio	Passive	——	1.13	——

[a]Range outside training range. [b]Training range of approximating analyzers. [c]Restricted range inside training range.

Table 3 Optimum weight for HSCT for the five test cases

	NASA CometBoards solution		Industry solution	
Test cases	Weight, lb	Deviation, %	Weight, lb	Deviation, %
1	666,529	0.0	678,450	1.8
2	666,578	0.0	666,730	0.0
3	677,264	1.6	667,064	0.1
4	666,526	0.0	666,658	0.0
5 (benchmark)	666,531	0.0	666,665	0.0

3) Landing approach velocity v_a, which must not exceed 160 kn:

$$g_3 = (v_a/160) - 1 \leq 0$$

4) Takeoff field length l_t, which must not exceed 11,000 ft:

$$g_4 = (l_t/11{,}000) - 1 \leq 0$$

5) Jet velocity v_j, which must not exceed 2300 kn:

$$g_5 = \frac{v_j}{2300} - 1 \leq 0$$

6) Compressor discharge temperature T, which must not exceed 1710°R:

$$g_6 = (T/1710) - 1 \leq 0$$

The constraints extracted from the FLOPS analyzer output in the soft-coupling process were passed into the CometBoards design test bed. Although the problem has several passive constraints, they were excluded from the design optimization calculations.

Benchmark Solution for the HSCT Aircraft

NASA Langley Research Center posed six test cases with different starting points and variable bounds for the HSCT aircraft problem.[23] NASA Lewis Research Center, using the CometBoards test bed and the FLOPS analyzer, obtained solutions for five of these cases, as did an industrial partner using its own optimizer and the FLOPS analyzer. Table 3 gives the optimum weights of the aircraft under the five different conditions, as obtained by the NASA Lewis Research Center and the industrial partner.

Case five is considered the benchmark solution against which all results, including neural network and regression answers, were compared. For the five cases given in Table 3, the gross takeoff weight of the HSCT aircraft obtained by the two groups agreed within a maximum deviation of 1.8%. Overall, these results, with minor derivations, can be considered acceptable, because aircraft optimization is a difficult problem. The problem may be difficult because of the variation in the constraints over a wide range and because of the empirical equations and smoothing techniques used in the FLOPS code. The weight, design variables, and constraints for the optimal solution of the benchmark case are given in Table 4.

The optimum solutions (see Table 4) were in agreement, with minor deviations, except for the second-segment climb thrust. However, both values of this constraint, which must be positive, are acceptable. The number of reanalyses required for the CometBoards and industry solutions (134 and 1240, respectively) differed because the industrial partner used a combination of a gradient-based algorithm along with a genetic code, which, for this problem, was computationally intensive. The optimum solution has also been verified graphically. At

Table 4 Benchmark solution for the HSCT aircraft

Parameters	Initial design	CometBoards solution	Industry solution
	Merit function		
Aircraft Weight, lb	793,395	666,531	666,665
	Active design variables		
(1) Engine thrust, lb	50,000.0	41,418.00	41,495.00
(2) Wing size, ft^2	7,000.0	8,170.00	8,162.00
(3) Turbine inlet temperature, °R	3,200.0	2,958.00	2,958.00
(4) Overall pressure ratio	18.0	21.62	21.63
(5) Bypass pressure ratio	0.7	0.43	0.44
(6) Fan pressure ratio	2.5	3.62	3.59
	Behavior constraints		
(1) Missed approach thrust, lb	87,718	71,029	71,174
(2) Second-segment climb thrust, lb	12,968	25	279
(3) Landing approach velocity, kn	169	147	147
(4) Takeoff field length, ft	13,742	11,000	11,000
(5) Jet velocity, kn	2,108	2,300	2,288
(6) Compressor discharge temperature, °R	1,587	1,710	1,710
Number of reanalyses to solution	——	134	1,240

optimum there are three active constraints: takeoff field length, jet velocity, and compressor discharge temperature.

Generation of the I/O Pairs for Training

The training data were generated in two steps. In the first step, the input portion of the I/O pairs was generated through the selection strategy illustrated earlier; it was calculated by using $bw = 3$ and by setting the number of stations between the initial design and both the lower or upper bound equal to four. The number of pseudorandom perturbations in the four intervals beginning with the initial design and moving toward the lower or upper bound are 40, 36, 32, and 28. This selection strategy biases the training set toward the initial design. The passive design variables were not altered. The selection strategy for the specified parameters yielded a total of 641 design variable input sets.

In the second step, for each of the 641 sets, the FLOPS aircraft analyzer was run to obtain 641 sets of response parameters consisting of the merit function and the behavior constraints. Examination of the FLOPS response parameters indicated that many of these could not be used for training. The reasons for these sets being categorized as nonusable were 1) the FLOPS analyzer encountered numerical instability, producing "NaN's" (not-a-numbers, three such occurrences); 2) the analyzer aborted without any ouput (14 occurrences); and 3) the analyzer encountered out-of-range conditions (212 occurrences). Of the 641 output sets, 229 sets could not be used. The 412 satisfactory design sets, which exceed the number of design variables by a factor of 35, were used for regression and neural network training. The bad design points sometimes interfere with the optimization process when the FLOPS analyzer is used directly. Such an analyzer deficiency suggests that the use of approximation methods might be beneficial in the design optimization of the HSCT aircraft. During the iterative design process, the optimizer can request prediction of the behavior parameters for design points that fall outside the valid range of the analyzer and cause instabilities. It is not evident that such instabilities can be eliminated by adjusting the optimization parameters, particularly with the use of the multidisciplinary analysis code FLOPS. Irrespective of their performance, neural network and regression methods extend predictions beyond the valid range, thereby circumventing instabilities.

Regression Approximations

Cubic polynomials in design variables and quadratic polynomials in reciprocal design variables were used for the regression analysis. An HSCT aircraft with six active design variables has 111 terms in the regression series, so that 412 training pairs is considered an adequate number for the regression function. The regression coefficients were determined by using the linear least-squares routine DGELS from the Lapack subroutine library.[33] Once the coefficients were known, Eq. (2) was used for functional approximations and Eqs. (3) and (4) for gradient calculations.

Neural Network Approximations

The 412 I/O pairs were separated into a set of 392 training pairs and 20 validation pairs. The neural network training used a Gaussian radial function for the merit function and all the constraints, except the second one (second-segment climb thrust), which used linear, polynomial, and reciprocal basis functions. The configuration parameters associated with the Gaussian radial function used were an initial threshold value of 0.15; a maximum of four threshold iterations; a threshold step size of 0.2; and a measure of the clustering algorithm control parameter α equal to 0.6 for the constraints, and 0.5 for the merit function.

Representative Response Predictions

The overall performance of neural network and regression analysis can be illustrated by considering the weight of the HSCT aircraft as an example. The aircraft weights obtained with approximation methods and the FLOPS analyzer are projected into two-dimensional planes with aircraft weight as a function of engine thrust in Fig. 4a and as a function of wing area in Fig. 4b. These two graphs reveal several attributes of the two approximating methods. Consider first the engine thrust within the training (or standard) range of 36,000–45,000 lb (Fig. 4a). In this figure for the engine thrust, the maximum error in the weight determined by the regression method is 4.6%, whereas that determined by the neural network is 3.7%. For both methods the errors peak at the lower boundary of this range. For the wing area in the standard range of 7100–9100 ft^2 (Fig. 4b), the maximum error obtained with the regression method was about 1.3%, and with the neural network it was about 3.4%. The error for the wing area variable peaks near the lower boundary with the regression method, but the neural network maximum error of 3.4% occurs at a wing area of about 8000 ft^2, which is inside the standard range. For both wing area and thrust, the aircraft weight approximation by the two methods shows substantial deviation outside the training (standard) range, as expected. Beyond the training range, the neural network performs somewhat better than the regression

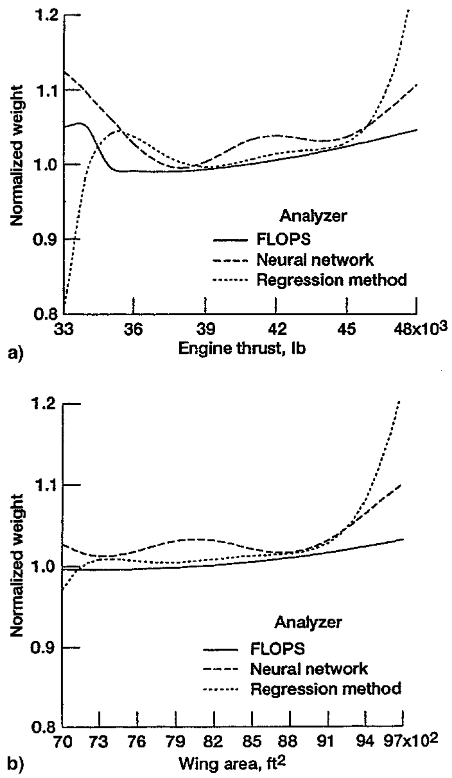

Fig. 4 Aircraft weights obtained by using approximations and FLOPS analyzer as a function of a) engine thrust and b) wing area.

method (see Fig. 4). In the standard range, both regression and neural network methods perform satisfactorily.

Analysis of the HSCT Aircraft by Approximation Methods

The responses obtained for the aircraft by neural network and regression approximations were examined for a set of 100 design points in each of the three ranges (restricted, standard, and wide). The design points were not selected from the training data; rather they were selected at random in the specified ranges. An attempt was made to generate the response parameters for these design points with the FLOPS analyzer. As before, the FLOPS analyzer could not generate valid responses for all 100 design points. It produced 100, 39, and 33 acceptable sets of response parameters in the restricted, standard, and wide ranges, respectively. Neural network and regression results in the three ranges were compared with only the acceptable sets from the FLOPS analyzer. The means of the relative absolute errors in the weight and in each constraint are presented in Table 5 for the three ranges.

Overall, Table 5 shows that the responses generated for the aircraft with both approximation methods progressively degrade from the restricted to the wide range. In the restricted range, approximations by regression analysis can be considered satisfactory, except for the second-segment climb thrust (the second constraint). For this constraint, the 3.4% error by regression analysis reduced to a 2.4% error by neural network analysis. To a certain extent, the discrepancy in this constraint can be attributed to the small number (around 25 lb) being normalized with respect to 10,000 lb. For example, an error of 25 lb in the second-segment climb thrust constraint, though physically negligible with respect to its bound of 10,000 lb, leads to a very large relative error of 100%. If this constraint were associated with a few hundred pounds of thrust, then a relative error of several fold would be seen, but it could still be inconsequential. A similar anomaly is observed in the benchmark solution for the second-segment climb thrust given in Table 4. CometBoard's (25 lb) and industry's (279 lb) solutions for the constraint differed by a factor of 11.4, but the variation is inconsequential. The performance of the neural network in the restricted range can be considered satisfactory except for the takeoff field length constraint. For this constraint, the 5.2% error by the neural network method reduced to a 1.8% error with regression analysis. The maximum error in the restricted range was about 5% for all the variables and constraints. In this range neural network and regression approximations complement each other.

In the standard range, the errors were substantially larger than in the restricted range. For example, both neural network and regression analysis showed an error of around 13.5% for the takeoff field length constraint. In this range, the regression and neural network approximation methods performed at about the same level, with the exception of the jet velocity constraint, for which regression analysis outperformed the neural network method. In the wide range, both the approximations exhibited higher errors. The error from the neural network was substantially lower than that of the regression method. An attempt was made to improve the regression method by replacing the basis functions with quadratic polynomials in the design variables only. (These results are given in the column marked "quadratic" in Table 5.) Even though using quadratic polynomials reduced the error in the regression approximation, the response still cannot be considered satisfactory. In the wide range, the performance of the regression method with quadratic polynomials can be considered similar to the performance of the neural network method, but neither is satisfactory.

In all three ranges, the regression approximation method (with a suitable choice of polynomials) and the neural network method can be considered to perform similarly in predicting responses for the HSCT aircraft.

Design Optimization of the HSCT Aircraft Through Approximations

This section examines the performance of approximation methods in optimization of the HSCT aircraft. The sequential quadratic programming algorithm used earlier to generate the benchmark results was retained as the optimizer. This gradient-based optimizer requires not only the values of the merit function and constraints but also their design sensitivities. Such gradient information is available only by using finite differences when the FLOPS code itself is used as the analyzer in design optimization. However, both approximating analyzers provide closed-form sensitivities. Results were obtained by using these closed-form sensitivity formulas in the neural network and regression methods. The optimization was also repeated by using finite difference sensitivity calculations with both approximating analyzers. In total, five methods were used to obtain sets of optimal results for the HSCT problem: 1) the FLOPS analyzer with finite difference gradients, 2) the neural network analyzer with closed-form gradients, 3) the neural network analyzer with finite difference gradients, 4) regression analysis with closed-form gradients, and 5) regression analysis with finite difference gradients. The optimization was carried out in the restricted, standard, and wide ranges. Because a review of the results indicated satisfactory performance only in the restricted range (as might have been expected from the results obtained for analysis validation), only those results are given in this section. Results for the other two ranges are provided in the Appendix. Table 6 summarizes the results generated for the five cases, along with the benchmark solutions obtained by using a closed-form gradient. Results were similar, with minor deviations, when finite difference gradients were used.

In the following paragraphs, the design variables, merit function, active constraints, and passive constraints are each discussed separately with respect to the performance of the approximation methods in design optimization.

Table 5 Percent mean error in three ranges

Response quantities	Restricted range: Regression method	Restricted range: Neural network	Standard range: Regression method	Standard range: Neural network	Wide range: Regression method, Cubic function	Wide range: Regression method, Quadratic function	Wide range: Neural network
Weight	0.4	0.9	2.2	2.6	1375	7.1	6.7
Missed approach	0	0.1	0.3	0.3	128	0.5	3.4
Second-segment climb	3.4	2.4	17.2	10.2	9720	110	110
Approach velocity	0.2	0.5	1.1	1.5	753	0.4	7.0
Takeoff field length	1.8	5.2	13.5	13.6	8180	109	65.8
Jet velocity	0.2	0.7	0.5	3.0	157	0.9	9.8
Compressor temperature	0.3	0.6	1.9	1.8	53	2.4	7.3

(All values: Mean error, %)

Table 6 HSCT aircraft design using approximations in restricted range with closed-form gradients

Design parameters	Benchmark solution	FLOPS analyzer	Neural network		Regression	
		Percent deviation in optimum solution				
Merit function						
Aircraft weight, lb	666,531	0.1	0.8	0.2[a]	1.0	0.7[a]
Active design variables						
Engine thrust, lb	41,418.00	0.0	−2.2	−2.2	0.2	0.2
Wing size, ft^2	8,170.00	0.1	0.3	0.3	1.3	1.3
Turbine inlet temperature, °R	2,958.00	−0.7	1.8	1.8	1.8	1.8
Overall pressure ratio	21.62	−2.1	−3.5	−3.5	−5.4	−5.4
Bypass pressure ratio	0.43	−6.2	3.3	3.3	7.6	7.6
Fan pressure ratio	3.62	−1.7	5.0	5.0	1.2	1.2
Behavior constraints						
Missed approach thrust, lb	71,029	−0.1	−3.7	−3.8[a]	−0.1	0.1[a]
Second-segment climb thrust, lb	25	−100.0	1706.0	−99.9[a]	760.8	−99.9[a]
Landing approach velocity, kn	147	−0.0	−0.1	−0.1[a]	−0.2	−0.3[a]
Takeoff field length, ft	11,000	0.1	0.0	4.7[a]	0.0	0.0[a]
Jet velocity, kn	2,300	−0.5	0.0	0.9[a]	0.0	0.4[a]
Compressor discharge temperature, °R	1,710	0.0	0.0	−1.0[a]	−1.8	−2.2[a]

[a]Values were generated by FLOPS analyzer for the optimum designs that were obtained by neural network and regression methods.

Design Variables

Notice that even when the FLOPS analyzer itself is used, the maximum deviation in the optimum values of the design variables exceeds 6% of the benchmark results. This deviation can be attributed to the nonlinearity of the eight disciplines within the FLOPS code, which uses statistical and empirical calculations to estimate the merit function and constraints. The optimum results with the neural network analyzer differed from the benchmark solution by a maximum of 5%. And the regression analyzer results differed by 7.6%. These maximum deviations of 5 and 7.6% are comparable to the 6% deviation for the FLOPS analyzer. Thus, the three analyzers (FLOPS, neural network, and linear regression) performed at about the same level.

Merit Function

The aircraft weights determined by the three analyzers deviated from the benchmark solution by a maximum of 1%. When the values of the design variables obtained with the regression scheme were used in the FLOPS code to calculate the weight, the error in the optimal weight decreased by 30% (from 1.0 to 0.7%). Similarly, the error reduction achieved by using the FLOPS code with the design from the neural network scheme was 75% (from 0.8 to 0.2%). Overall, for the HSCT problem the three analysis methods performed at about the same level.

Active Constraints

The benchmark solution has three active constraints: takeoff field length, jet velocity, and compressor discharge temperature. Optimization with the FLOPS analyzer produced the same active set within a 0.5% deviation. The neural network optimization results contained the same three active constraints. When the neural network optimum design was used with the FLOPS analyzer to back-calculate these constraints, the jet velocity and compressor discharge temperature agreed within 1%. However, the takeoff field length was infeasible at about 5% deviation. Optimization with regression analysis also produced the same set of active constraints, with a 2% deviation for the compressor discharge temperature. When the regression optimum design was used with the FLOPS analyzer to back-calculate the active constraints, the takeoff field length and jet velocity agreed within 0.4% deviation. The deviation in the compressor discharge temperature was about 2%. Although the approximating analyzers often returned with active constraint values of 0.0, this can be deceptive because these values are only an approximation of the true values. The actual constraint values obtained with the original FLOPS code are given in Table 6.

Passive Constraints

The benchmark solution has three passive constraints: missed approach, second-segment climb thrust, and landing-approach velocity. The missed approach and landing-approach velocity constraints agreed with the benchmark solutions within a 0.1% deviation when the FLOPS analyzer was used. However, the second-segment climb constraint became active, which caused a 100% deviation, corresponding to a 0-lb thrust (vs the 25-lb benchmark solution). Both of these amounts are small compared to the 10,000 lb normalization factor, as discussed earlier. The neural network optimization returned the same three passive constraints, with a maximum deviation of about 4% for the missed approach thrust and landing approach velocity. The second-segment climb thrust determined with the neural network deviated by 1706%, which represents 443 lb; this too can be considered small compared with 10,000 lb. When the neural network optimum design was used with the FLOPS analyzer to back-calculate these constraints, the missed approach thrust and landing-approach velocity constraints agreed with the neural network-generated constraint values. In this case, the deviation between FLOPS and the neural network method for the second-segment climb constraint represents 25 lb, which can also be considered relatively small compared with the normalization factor. The regression optimization also returned the same three passive constraints, with a maximum deviation of less than 0.2% for the missed approach thrust and the landing approach velocity. It produced a deviation of 761% for the second-segment climb, which represents 211 lb, a relatively small amount compared with 10,000 lb. When the regression method optimum design was used with the FLOPS analyzer to calculate these constraints, the missed approach thrust and landing approach velocity constraints agreed with the regression-generated constraint values reasonably well. The deviation between the FLOPS and regression values for the second-segment climb constraint represents 25 lb, which can also be considered relatively small compared to its normalization factor. Thus, the neural network and regression analysis methods can both be considered to have performed satisfactorily in determining the values of the passive constraints, though the regression scheme was slightly better.

Influence of Gradient Generation Schemes in Design Optimization of HSCT Aircraft

The results presented in Table 6, which were obtained by using closed-form gradients, were generated again with finite difference gradients. The regression and neural network methods produced optimization results that were similar, whether by closed-form or finite difference gradients. For the aircraft weight, both methods gave about the same results. Using the two gradient approaches with the regression method produced results almost identical to the optimum values of the design variables. With the neural network method, the maximum deviation of these variables was less than 2%. Constraint values, with the exception of the second-segment climb thrust, follow the same pattern. For this passive constraint, the neural network deviation represents 316 lb, which, as before, can be considered small compared to the normalization factor of 10,000 lb.

CPU Time for Design Optimization

The CPU times associated with design optimization of the HSCT aircraft are given in Table 7. A Silicon Graphics Power Series 480-VGX with eight 40-MHz processors and 256 Mbytes of main memory was used for all the calculations. The total time is separated into user and system component times.

Table 7 CPU time for design optimization on a Silicon Graphics PS 480-VGX[a]

	FLOPS		Neural network				Regression analysis			
	Closed-form gradients		Closed-form gradients		Finite difference gradients[b]		Closed-form gradients[b]		Finite difference gradients[b]	
Activity	User	System	User	System	User	System	User	System	User	System
Generation of I/O pairs	——	——	63,207	827	(a)	(b)	(a)	(b)	(a)	(b)
Training	——	——	2,407	16.8	(c)	(d)	2.2	0.2	(e)	(f)
Optimization	8,897	96	24.1	40.3	124.4	263.5	0.4	0.1	1.9	0.2

[a]All times are given in seconds.
[b](a) and (b) generation of I/O pairs was carried out only once; (c) to (f) neural network and regression methods were trained once.

Table 8 HSCT aircraft design using approximations in standard range with closed-form gradients

		Percent deviation in optimum solution				
Design parameters	Benchmark solution	FLOPS analyzer	Neural network		Regression	
		Merit function				
Aircraft weight, lb	666,531	0.0	−1.2	0.1[a]	−10.8	1.6[a]
		Active design variables				
Engine thrust, lb	41,418.00	−0.1	−4.5	−4.5	−13.1	−13.1
Wing size, ft^2	8,170.00	0.1	−2.6	−2.6	−13.1	−13.1
Turbine inlet temperature, °R	2,958.00	−0.2	2.8	2.8	3.3	3.3
Overall pressure ratio	21.62	−1.2	−3.9	−3.9	13.7	13.7
Bypass pressure ratio	0.43	−6.4	10.0	10.0	84.3	84.3
Fan pressure ratio	3.62	−0.6	10.2	10.2	−7.9	−7.9
		Behavior constraints				
Missed approach thrust, lb	71,029	−0.1	−6.7	−7.9[a]	−11.6	−26.6[a]
Second-segment climb thrust, lb	25	20.8	1907.7	−99.9[a]	76,827.0	−100.0[a]
Landing approach velocity, kn	147	0.0	0.5	1.3[a]	2.2	8.1[a]
Takeoff field length, ft	11,000	0.0	0.0	12.7[a]	−3.8	67.8[a]
Jet velocity, kn	2,300	0.0	0.0	0.9	−12.9	−9.8[a]
Compressor discharge temperature, °R	1,710	0.0	0.0	1.0[a]	0.0	1.6[a]

[a]Values were generated by FLOPS analyzer for the optimum designs that were obtained by neural network and regression methods.

The user component is primarily computation time. The system component, which is typically small, accounts for forking of processes as well as some manipulation of files. The relatively large system times in Table 7 can be attributed to soft-coupling of the CometBoards, Cometnet, and FLOPS codes. Generation of the I/O pairs consumed the most time (almost 18 h). Neural network training took about 0.67 h, but regression analysis training time was negligible. Regular optimization with the FLOPS code itself required 2.5 h (when the process was successful). Neural network-based optimization took 1 min when closed-form sensitivities were used, but the time increased to 6.5 min when finite difference gradients were used. For regression analysis with closed-form gradients, the time for optimization was less than 1 s, but it increased to 2 s when numerical sensitivities were used. The user CPU times for optimization with closed-form gradients via neural network and regression methods were 24.1 s and 0.4 s, respectively. Even if a portion of the neural network time can be attributed to soft-coupling, it is unlikely that the time can be reduced from 24.1 s to less than 0.4 s.

Optimization by approximation methods substantially reduced the computation time in comparison to regular optimization. The reduction factor was 140 when a neural network was used with closed-form gradients, and it was almost 18,000 when regression analysis was used. Although these reduction factors are attractive, keep in mind that the I/O-pair generation and training times were 18.5 and 17.8 h for neural network and regression methods, respectively. Overall, for the HSCT aircraft problem, regular optimization time, which has been measured in hours, was reduced to minutes with a neural network and to seconds with a regression scheme; however, a substantial price was paid for the generation of the derived approximating analyzers. The approximation methods, despite the training penalty, can be advantageous for situations in which the aircraft design solution is required multiple times with minor variations in constraints and design parameters.

Optimization worked satisfactorily with closed-form as well as numerical gradients. Numerical sensitivities, however, increased the solution time by factors of 6.0 and 4.2 for the neural network and regression methods, respectively.

Note that using approximation methods to solve an optimization problem required the separation of bad response points from the candidate I/O pairs generated by the FLOPS code. The time required for this operation is not included in this discussion.

Summary of Results

The regular design optimization capability of CometBoards has been augmented with two approximation methods: neural network and regression analysis. This paper presents the validation of the approximation methods for the analysis and design of an HSCT aircraft. Intensive computation in the optimization of the aircraft was reduced by using the neural network and regression approximation methods. Regular CPU time for aircraft optimization has been measured in hours but was reduced to minutes with a neural network and to seconds with the regression scheme. The regression and neural network methods can be considered to have performed satisfactorily within an appropriate range for both the analysis and design of the aircraft. When the derived analyzers used closed-form gradients, the computation time for optimization was further reduced. Both approximation methods eliminated the effect of the instability in the FLOPS code that can interfere with the optimization process and lead to premature termination. Generation of the derived analyzers for both the neural network and regression methods required substantial computational time. Training time for the regression method was negligible. The aircraft problem required that training be done in a large (standard) range and optimization be performed in a smaller (restricted) range. The training and optimization ranges should be strategized prior to developing the derived analyzers.

Overall, neural network and regression approximation methods were found satisfactory for the analysis and design optimization of a HSCT aircraft.

Appendix: HSCT Aircraft Optimum Solutions in the Standard and Wide Ranges

The optimum solutions for the HSCT design in the standard and wide ranges are summarized in this Appendix. Both closed-form gradients and finite difference gradients were used to obtain the solutions. The solution in the standard range is presented in Table 8. The solutions in all three ranges (standard, wide, and restricted) are compared with the benchmark solution in a bar chart format in Figs. A1 and A2. The performance of the approximation methods in design optimization of the HSCT aircraft in the standard and wide ranges is discussed separately with respect to the design variables, merit function, active constraints, and passive constraints.

Design Variables

The optimum results for the first four design variables (thrust, wing area, inlet temperature, and overall pressure ratio) as determined with the neural network analyzer differed from the benchmark solution by a maximum of 5% in the standard and wide ranges (see Fig. A1). The maximum deviation obtained by this method for the other two design variables (bypass and fan pressure ratios) was 10% in the standard range

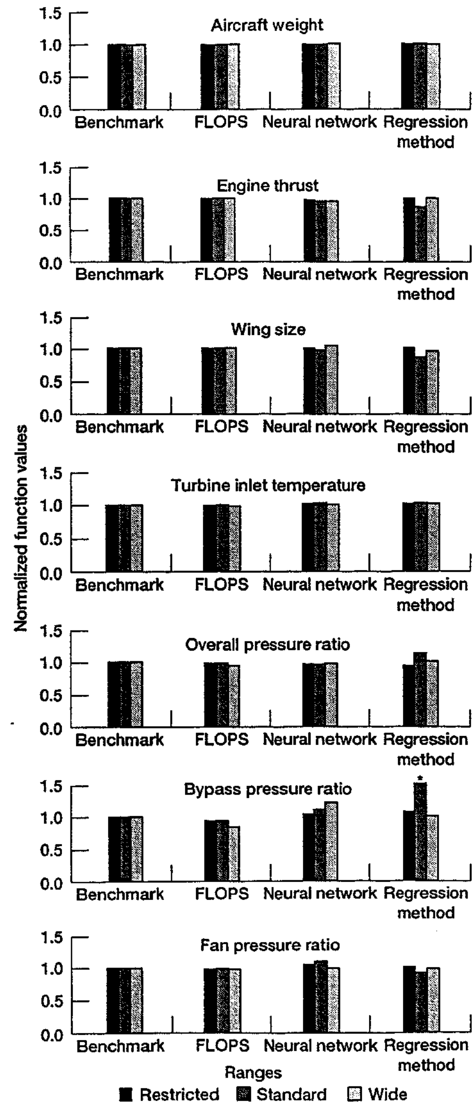

Fig. A1 Normalized optimum weight and six design variables for HSCT aircraft. (*Truncated.)

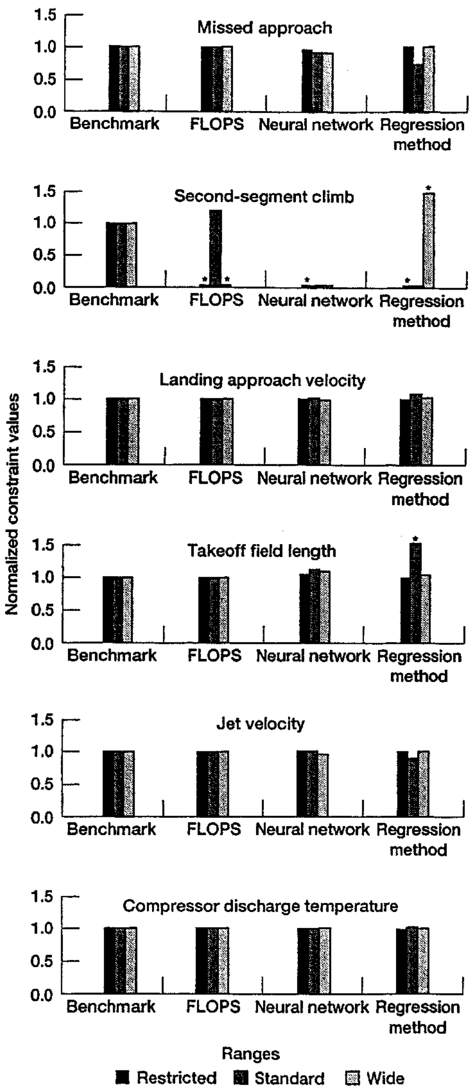

Fig. A2 Normalized constraint values at the optimum for HSCT aircraft. (*Padded or truncated.)

and 21% in the wide range. Using the regression method in the standard range yielded a maximum deviation for the design variables within 14%, except for the bypass pressure ratio, which was about 84%. The performance of the full cubic polynomial regression method was unacceptable in the wide range. Thus, the regression approximator was retrained with a quadratic polynomial in the design variables. In the wide range, the maximum deviation for the design variables was within 4% by this method.

Merit Function

The merit function was better behaved than the design variables in both ranges, except for an 11% deviation obtained by the regression method in the standard range (Fig. A1).

Active Constraints

With the neural network method, the maximum deviation of the active constraints in both ranges was within 13%. With the regression method, the maximum deviation of 68% in the standard range was reduced to 4% when the regression approximator was retrained with quadratic basis functions in the wide range (see Fig. A2).

Passive Constraints

A large deviation was observed for the passive constraints in both the standard and wide ranges. For example, the second-segment climb thrust as determined by the neural network deviated by 1907%, and that determined by the regression method deviated by 76,827%. This constraint exhibited substantial deviation in the restricted range; however, its performance in the standard and wide ranges is considered unacceptable (see Fig. A2).

The regression and neural network methods gave similar optimization results, with some deviations, regardless of whether closed-form or finite difference gradients were used.

References

[1]Guptill, J. D., Coroneos, R. M., Patnaik, S. N., Hopkins, D. A., and Berke, L., "CometBoards Users Manual: Release 1.0," NASA TM-4537, Oct. 1996.

[2]Patnaik, S. N., Coroneos, R. M., Guptill, J. D., and Hopkins, D. A., "Comparative Evaluation of Different Optimization Algorithms for Structural Design Applications," *International Journal for Numerical Methods in Engineering*, Vol. 39, Jan. 1996, pp. 1761–1774.

[3]Patnaik, S. N., Guptill, J. D., and Berke, L., "Singularity in Structural Optimization," *International Journal for Numerical Methods in Engineering*, Vol. 36, No. 6, 1993, pp. 931–944.

[4]Patnaik, S. N., Lavelle, T. M., Hopkins, D. A., and Coroneos, R. M., "Cascade Optimization Strategy for Aircraft and Air-Breathing Propulsion System Concepts," *Journal of Aircraft*, Vol. 34, No. 1, 1997, pp. 136–139.

[5]McCullers, L. A., "Aircraft Configuration Optimization Including Optimized Flight Profiles," *Recent Experiences in Multidisciplinery Analysis and Optimization*, edited by J. Sobieski, Pt. 1, NASA CP-2327, Jan. 1984.

[6]Patnaik, S. N., Guptill, J. D., and Berke, L., "Merits and Limitations of Optimality Criteria Method for Structural Optimization," *International Journal for Numerical Methods in Engineering*, Vol. 38, No. 18, 1995, pp. 3087–3120.

[7]"DOT User's Manual, Version 2.00," Engineering Design Optimization, Inc., Santa Barbara, CA, 1989.

[8]Belegundu, A. D., Berke, L., and Patnaik, S. N., "An Optimization Algorithm Based on the Method of Feasible Directions," *Structural Optimization*, Vol. 9, No. 2, 1995, pp. 83–88.

[9]Schittkowski, K., "User's Manual, FORTRAN Subroutines for Mathematical Applications, Version 2.0," IMSL, Inc., Houston, TX, 1991.

[10]Arora, J. S., "IDESIGN User's Manual Version 3.5.2," Optimal Design Lab., Univ. of Iowa, Iowa City, IA, 1989.

[11]"NAG FORTRAN Library Manual—MARK 15," NAG FORTRAN Library Routine Document, Downer's Grove, IL, 1991.

[12]Miura, H., and Schmit, L. A., Jr., "NEWSUMT: A FORTRAN Program for Inequality Constrained Function Minimization, Users Guide," NASA CR-159070, June 1979.

[13]Gabriele, G. A., and Ragsdell, K. M., "OPT—A Nonlinear Programming Code in FORTRAN Implementing the Generalized Reduced Gradient Method, User's Manual," University of Missouri, Columbia, MO, 1984.

[14]"RPK_NASTRAN," COSMIC, Univ. of Georgia, Athens, GA, 1994.

[15]Nakazawa, S., "MHOST Version 4.2, Vol. 1: User's Manual," NASA CR-182235, Jan. 1989.

[16]Venkayya, V. B., and Tischler, V. A., "ANALYZE: Analysis of Aerospace Structures with Membrane Elements," Air Force Flight Dynamics Lab., AFFDL-TR-78-170, Wright–Patterson AFB, OH, Dec. 1978.

[17]Patnaik, S. N., Hopkins, D. A., Aiello, R. A., and Berke, L., "Improved Accuracy for Finite Element Structural Analysis via a New Integrated Force Method," NASA TP-3204, April 1992.

[18]Plencner, R. M., and Snyder, C. A., "The Navy/NASA Engine Program (NNEP89): A User's Manual," NASA TM-105186, Aug. 1991.

[19]Gendy, A. S., Patnaik, S. N., Hopkins, D. A., and Berke, L., "Parallel Computational Environment for Substructure Optimization," NASA TM-4680, Dec. 1995.

[20]Hafez, W. A., "Cometnet—User Manual," IntelliSys, Beachwood, OH, 1996.

[21]Feagin, R. C., and Morrison, W. D., "Delta Method, an Empirical Drag Buildup Technique," NASA CR-151971, Dec. 1978.

[22]Sommer, S. C., and Short, B. J., "Free-Flight Measurements of Turbulent-Boundary-Layer Skin Friction in the Presence of Severe Aerodynamic Heating at Mach Numbers from 2.8 to 7.0," NACA TN-3391, March 1955.

[23]Geiselhart, K. A., "A Technique for Integrating Engine Cycle and

Aircraft Configuration Optimization," NASA CR-191602, Feb. 1994.

[24]Geiselhart, K. A., Caddy, M. J., and Morris, S. J., Jr., "Computer Program for Estimating Performance of Air-Breathing Aircraft Engines," NASA TM-4254, May 1991.

[25]Caddy, M. J., and Shapiro, S. R., "NEPCOMP: The Navy Engine Performance Computer Program, Version I," NADC-74045-30, April 1975.

[26]Clark, B. J., "Computer Program to Predict Aircraft Noise Levels," NASA TP-1913, Sept. 1981.

[27]Johnson, V. S., "Life Cycle Cost in the Conceptual Design of Subsonic Commercial Aircraft," Ph.D. Dissertation, Univ. of Kansas, Lawrence, KS, 1988.

[28]Eide, D. G., "Cost Estimating Relationships for Airframes in the Development and Production Phases," NASA TM-80229, June 1980.

[29]Beltramo, M. N., Trapp, D. L., Kimoto, B. W., and Marsh, D. P., "Parametric Study of Transport Aircraft Systems Cost and Weight," NASA CR-151970, April 1977.

[30]Nelson, J. R., and Timson, F. S., "Relating Technology to Acquisition Costs: Aircraft Turbine Engines," RAND Corp., R-1288-PR, Santa Monica, CA, March 1974.

[31]"A New Method for Estimating Current and Future Transport Aircraft Operating Economics," American Airlines, NASA CR-145190 (revised), March 1978.

[32]Stoessel, R. F., "A Proposed Standard Method for Estimating Airline Indirect Operating Expense," Lockheed Martin Corp., Marietta, GA, 1970.

[33]Anderson, E., Bai, Z., Bischof, C., Demmel, J., Dongarra, J., DuCroz, J., Greenbaum, A., Hammarling, S., McKenney, A., Ostrouchov, S., and Sorensen, D., "LAPACK User's Guide," Society for Industrial and Applied Mathematics, Philadelphia, PA, 1992.

[34]Vetterling, W. T., Press, W., Teukolsky, S., and Flannery, B., "Numerical Recipes Example Book (C)," Cambridge Univ. Press, New York, 1987.

[35]Rissanen, J., "Stochastic Complexity," *Journal of the Royal Statistical Society, Series B—Methodological*, Vol. 49, No. 3, 1987, pp. 223–239.